ELSEVIER

Contents lists available at ScienceDirect

Materials Today Sustainability

journal homepage: https://www.journals.elsevier.com/ materials-today-sustainability



Eco-friendly passive radiative cooling using recycled packaging plastics



Y. Liu ^a, X. Liu ^a, F. Chen ^a, Y. Tian ^a, A. Caratenuto ^a, Y. Mu ^a, S. Cui ^{b, c}, M.L. Minus ^a, Y. Zheng ^{a, *}

- ^a Department of Mechanical and Industrial Engineering, Northeastern University, Boston, MA 02115, USA
- ^b Department of Mechanical Engineering, University of Texas at Dallas, Richardson, TX 75080, USA
- ^c National Renewable Energy Laboratory, Golden, CO 80401, USA

ARTICLE INFO

Article history:
Received 27 September 2022
Received in revised form
11 May 2023
Accepted 26 June 2023
Available online 30 June 2023

Keywords:
Passive daytime radiative cooling
Low-cost and eco-friendly
Recycled polystyrene foam
High solar reflectivity
High lumidity

ABSTRACT

Passive daytime radiative cooling, requiring zero external energy consumption, is a promising cooling strategy achieved by simultaneously reflecting solar irradiance and thermally radiating heat into the cold outer space (~ 3 K) through the atmospheric transparency window. However, current materials for passive radiative cooling face huge challenges, such as complicated fabrication approaches, expensive raw materials, and environmental requirements for practical applications. In line with the urgent need for plastic recycling to curb global environmental pollution, the recycled plastics are used to fabricate a passive radiative cooling material. Herein, the foam-paper composite (FPC) with excellent self-cooling capability is fabricated by a simple crushing-and-mixing procedure using recycled polystyrene (PS) foam and printer paper. The superhydrophobic PS foam particles not only protect the FPC from water damage for field applications but also reinforce its solar reflectivity via their porous structure. The cellulose fibers in printer paper can efficiently emit infrared thermal radiation into the cold outer space and bond dispersed PS foam particles together, further increasing its mechanical strength. The combination of highly diffusely reflective PS foam particles and fiber-based printer paper results in a reflectivity of 96% in the solar spectrum, a sub-ambient cooling performance of 8.4 °C, and a maximum radiative cooling power of 90 W/m² during a 24-h cycle. Meanwhile, the FPC with high humidity can maintain its high solar reflectivity, which promotes its application in humid subtropical areas. Furthermore, the low material cost and ease of fabrication will provide a path for effective daytime radiative cooling, especially in less developed areas.

© 2023 Elsevier Ltd. All rights reserved.

1. Introduction

Conventional cooling systems based on the vaporization and compression of various refrigerants consumed about 10% of the total U.S. electricity consumption in 2021 [1]. This results in tremendous greenhouse gas emissions the environment, accelerating global warming [2]. Therefore, an eco-friendly and energy-saving cooling technology is in urgent demand for future applications. The passive radiative cooling (PRC) method can efficiently reflect sunlight (0.3 ~ 2.5 μm) and emit infrared thermal radiation to the cold outer space (~3 K) through the atmospheric transparent window (8 ~ 13 μm). These cooling processes occur simultaneously

and without any electricity input, which provides great opportunity for the reduction of energy consumption in various cooling applications [3–7]. To reduce their temperatures below ambient under direct sunlight, PRC structures should possess high solar reflectivity ($R_{\rm S}$) and high infrared thermal emissivity ($E_{\rm IR}$) simultaneously. In recent years, a variety of the pyridinium dichromate (PDC) structures have been proposed to successfully achieve sub-ambient temperatures under direct sunlight, including multilayer structures [8–10], metamaterials [11–15], randomly distributed particle structures [16–22], and porous structures [23–28]. Although these sub-ambient cooling structures have good performance, their design and fabrication are either complicated or costly, which has hindered wide-field applications for infrastructure.

Due to the exceptional performance of polymeric materials, the current global demand for plastics continues to rise and is expected to reach up to 417 million tons per year by 2030 [29,30]. One

^{*} Corresponding author. E-mail address: y.zheng@northeastern.edu (Y. Zheng).

byproduct of this trend is a dramatic increase in plastic waste. Promoting the reduction, reuse, and recycling of plastics will prevent the release of more polymeric materials into the environment and thus curb environmental pollution [31,32]. At present, mechanical recycling is a main tool in an environmentally and economically sustainable economy of five main packaging plastics: polyethylene terephthalate (PETE), polyethylene (PE), polypropylene (PP), polystyrene (PS), and polyvinyl chloride (PVC) [33,34], which is still limited by cost mechanical degradation. Thus, mechanical-based strategies to improve their recycling value urgently need to be proposed. Printer paper is a commonly used office supply, in large part due to its abundance of raw materials and remarkable biodegradability. Printer paper has both high R_S and ε_{IR} due to the existence of cellulose fibers and the molecular vibrations of C-O and C-O-C bonds in cellulose, which makes it a good candidate material for PRC structures [21]. However, although printer paper possesses the passive radiative cooling property, its insufficient water resistance makes it inviable for field applications. Here, to provide a low-cost PDC material, printer paper and recycled PS foam are utilized to fabricate PDC structures to enrich their value and decrease environmental pollution (Fig. 1).

In this work, we theoretically and experimentally demonstrate effective daytime passive radiative cooling materials by employing recycled PS foams and cellulose-based papers that are ideal for performance in outdoor environments. We fabricate a foam-paper composite (FPC) via the crushing and mixing of PS foams and paper and experimentally test the optical and thermal properties of the FPC. Owing to the combination of the efficient scattering effects of the FPC's micropores and microfibers, the FPC exhibits a particularly high solar reflectivity of 96% (Fig. 3a). Meanwhile, the thermal performance and radiative cooling power of our fabricated FPC radiative coolers are also theoretically investigated for passive daytime cooling during a 24-h cycle. The calculation results validate a temperature decrease of up to 8.4 °C. In addition, we experimentally consider the effects of a humid environment on the optical properties and cooling performance. These theoretical and experimental findings open a promising path for effective daytime radiative cooling with low-cost and easy-to-fabricate materials, especially for less-developed areas.

2. Experimental section

2.1. Materials

20 lb paper is obtained from Hammermill Copy Plus Paper, and the PS foam is obtained from Dell Inc.

2.2. Methods

First, the printer papers (3 g, Hammermill Copy Plus Paper) were cut into small pieces and immersed in water for 1 h. After rinsing the recycled PS foams with deionized (DI) water, the PS foam board (3 g) was cut into small pieces and then addedto the paper pulp using a high-speed blender for 3 min (Vitamix E310). Assisted by the vacuum filtration, the following baking process accelerates the evaporation of water in the FPC with a thickness of ~ 1 cm. Then, the totally dry FPC was pressed into a thin sheet using a hydraulic press machine (DABPRESS, 10 tons) at 20 MPa. This forms a FPC sheet ($M_{\rm foam}/M_{\rm paper}$, F1:P1) with a diameter of 100 mm and a thickness of 2 mm (Fig. 2). As comparison, two FPC sheets with different mass ratios ($M_{\rm foam}/M_{\rm paper}$, F5:P1 and F1:P5, respectively) were also prepared to investigate how the mass ratio of these two materials affects the solar reflection and infrared emission abilities.

2.3. Morphology characterization

The surface morphologies of pressed FPC were examined by a scanning electron microscope (SEM, S5200, Hitachi Company) under an acceleration voltage of 3 kV.

2.4. Optical characterization

The reflectivity spectra (0.3 ~ 2.5 μm) were measured using a Jasco V770 spectrophotometer. The reflectivity spectra (2.5 ~ 20 μm) were measured using a Jasco FTIR 6600. Angular-dependent reflectivity spectra were measured using wedge blocks with different angles at the sample port of these two integrating spheres [21].



Fig. 1. Schematic illustrating the radiative cooling mechanism of the FPC and its closed-loop fabrication and recycling processes.

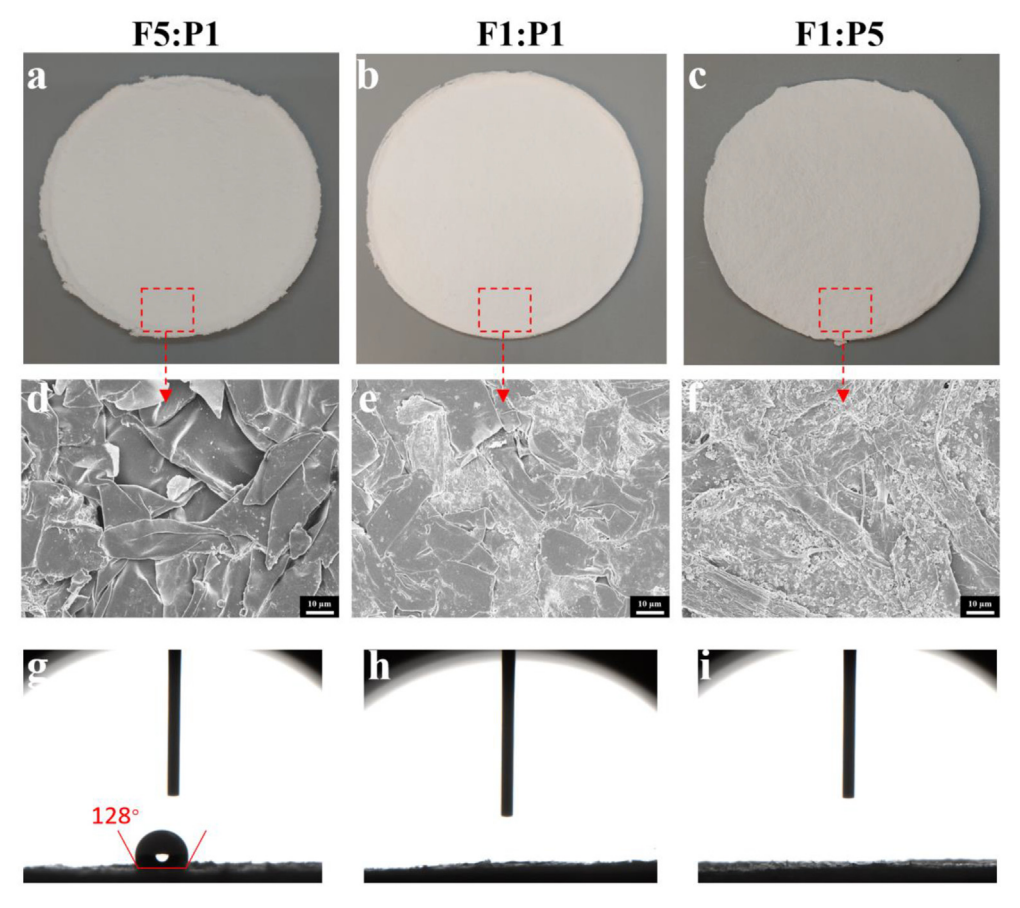


Fig. 2. (a-c) Optical images, (d-f) SEM images, and (g-i) water CA of the as-prepared 100 mm-diameter and 2 mm-thick FPC samples with different mass ratios, F5:P1, F1:P1, and F1:P5, respectively.

2.5. Thermal conductivity measurement

The thermal conductivities of FPC were measured by the thin-film module of the TPS 2500s.

2.6. Mechanical strength measurement

The mechanical strengths of the PFC thin sheet (10 cm \times 3 cm \times 2 mm) were measured using a dynamic mechanical analyzer (DMA) (RSA-G2, TA Instruments) at a constant strain rate. Compression test data were collected via TRIOS software (TA Instruments).

3. Results and discussion

According to our low-cost and eco-friendly requirements, we chose PS foams and printer papers to design the passive radiative cooling material owing to their beneficial features and recyclability. On the one hand, adding the printer paperto the FPC provides distributed cellulose fibers that can bond dispersed micro-PS foam particles together, further increasing its mechanical strength. On the other hand, PS foam particles possess excellent hydrophobicity, making the FPC more suitable for complex and dynamic outdoor conditions. Therefore, compared with the single PS foam board or printer paper, the combination of the PS foam particles and the fibers in printer paper provides an attractive candidate for passive radiative cooling materials for buildings. Fig. 2a—c shows the asprepared 10-cm-diameter and 2-mm-thick FPC samples with different mass ratios, F5:P1, F1:P1, and F1:P5, respectively, all

purely white under sunlight. We further visualize the morphology via scanning electron microscopy (SEM). These images show that the FPC consists of its internal porous and fibrous structures (Fig. 2d-f and S1). These interconnected microfibers assemble continuous boundaries between micropores, connecting the foam particles tightly together. The interfaces of the porous structure between PS foam particles and air voids enhance the photon scattering in the FPC film, thus increasing the overall solar reflectance. The effect of the press process on the porous structure and the solar reflectance of FPC is shown in Figs. S2 and S3, respectively. Meanwhile, the SEM images clearly display the microscopic changes brought on by different mass ratios between PS foam and paper. The increased ratio of PS foam will obviously increase pores on its top surface, further increasing the interfaces between PS foam particles and air voids, while the increase of paper will increase the interconnected microfibers on the boundaries. When the mass ratio is F5:P1, such a rough surface also has superior behavior in terms of water-repelling properties, as shown by high water contact angles of approximately 128° (Fig. 2g). As expected, the increased ratio of paper increases the top surface hydrophilicity, as shown in Fig. 2h and i.

We then investigated the absorptivity/emissivity between 0.3 and 20 μm and the mechanical strength of the FPC samples, as illustrated in Fig. 3. The absorptivity is calculated by subtracting the measured reflectivity from 1.0. The emissivity is then taken as absorptivity based on Kirchhoff's law of thermal radiation. The measured spectral reflectance of the FPC sample (F1:P1) indicates that the 2 mm thick film can reflect 96% of solar irradiation while possessing a high thermal emissivity of 0.80 between 8 and 13 μm

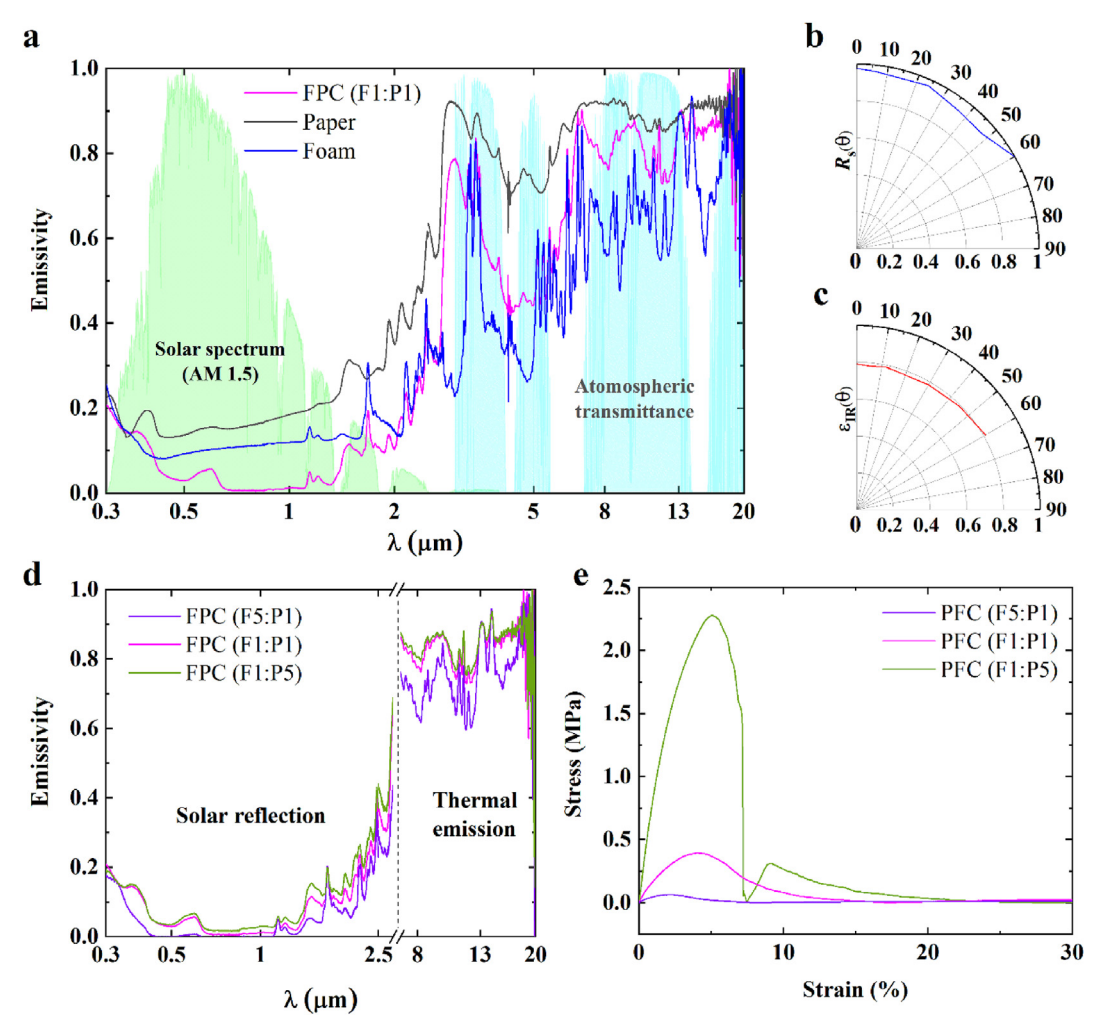


Fig. 3. (a) Hemispherical spectral emissivities of a 2-mm-thick FPC sample (F1:P1), printer paper, and PS foam board plotted against the normalized AM 1.5 spectrum (ASTM G173) and the atmospheric window, respectively. (b) high solar reflectivities and (c) thermal emissivities of the FPC sample at different angles of incidence. (d) hemispherical spectral emissivities and (e) stress-strain curves of FPC samples with different mass ratios.

(Fig. 3a). Interestingly, compared with the single PS foam and original printer paper, the R_S of the FPC is significantly enhanced from 0.80 (foam) to 0.96 (FPC). This result could be attributed to the increased interfaces of the porous structure between PS foam particles and air voids, which enhance the overall sunlight scattering of the FPC. Furthermore, the hierarchically randomized arranged PS foam particles and microfibers result in a high diffused R_S, which strongly backscatters sunlight regardless of the angle of incidence (0 \sim 60°; Fig. 3b). For the infrared thermal emissivity over the atmospheric transparent window (8 ~ 13 µm), an angleindependent high ε_{IR} of 0.80 is demonstrated due to the existence of the randomly stacked cellulose fibers in the FPC sample ($0 \sim 60^{\circ}$; Fig. 3c). Meanwhile, the mass ratio between the PS foam and printer paper will obviously affect the spectral absorptivity/emissivity distribution since the PS foam particles enhance the R_S of the FPC while the cellulose fibers will contribute to increases in the infrared thermal emissivity $\varepsilon_{\rm IR}$. In addition, the FPCs show increased tensile strength at higher mass ratios (Fig. 3e). Combining the water resistance and mechanical properties of the FPC samples, the FPC's mass ratio of 1:1 and excellent comprehensive performance suggest broader cooling applications in harsh environments.

To accurately evaluate the radiative cooling performance of the FPC, we establish the energy balance equation for a terrestrial radiative cooling device [22,35–37]:

$$Q_{\text{net}} = Q_{\text{FPC}}(T_{\text{FPC}}) - Q_{\text{sun}}(T_{\text{FPC}}) - Q_{\text{nr}}(T_{\text{amb}}, T_{\text{FPC}}) - Q_{\text{amb}}(T_{\text{amb}})$$

$$\tag{1}$$

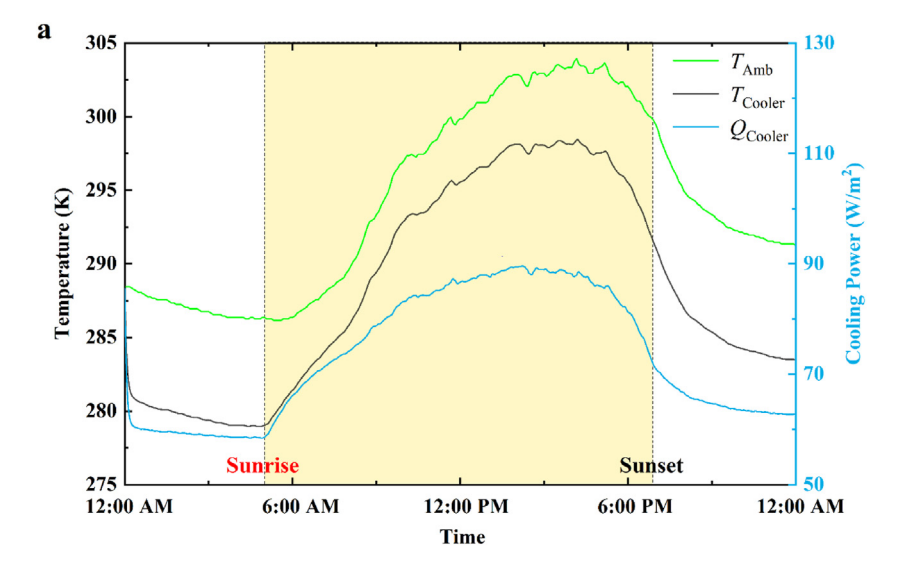
where $Q_{\rm net}$ and $Q_{\rm FPC}$ are the net cooling power and radiative power of the FPC, respectively. $Q_{\rm nr}$ accounts for the nonradiative heat transfer, $Q_{\rm amb}$ represents the incident thermal radiation from the atmosphere, and $Q_{\rm sun}$ is the incident solar power absorbed by the FPC. $T_{\rm amb}$ and $T_{\rm FPC}$ are the temperatures of ambient and FPC, respectively. $Q_{\rm FPC}$ is given by:

$$Q_{\text{FPC}}(T_{\text{FPC}}) = A \int_{0}^{\infty} d\lambda I_{\text{BB}}(T_{\text{FPC}}, \lambda) \varepsilon(\lambda, \theta, \varphi, T_{\text{FPC}})$$
 (2)

where $I_{\rm BB}(T_{\rm FPC}$, $\lambda) = 2hc^2\lambda^{-5}[\exp(hc/\lambda k_{\rm B}T)-1]^{-1}$ defines the spectral radiance of a blackbody. The non-radiative heat transfer between the ambient air and the FPC is determined as follows:

$$Q_{\rm nr}(T_{\rm amb}, T_{\rm FPC}) = Ah_{\rm nr}(T_{\rm amb} - T_{\rm FPC}) \tag{3}$$

where h_{nr} stands for the non-radiative heat transfer coefficient. Here, $h_{nr} = 8 \text{ Wm}^{-2}\text{K}^{-1}$ is used throughout the calculations [35,38,39]. $Q_{amb}(T_{amb})$ is given by



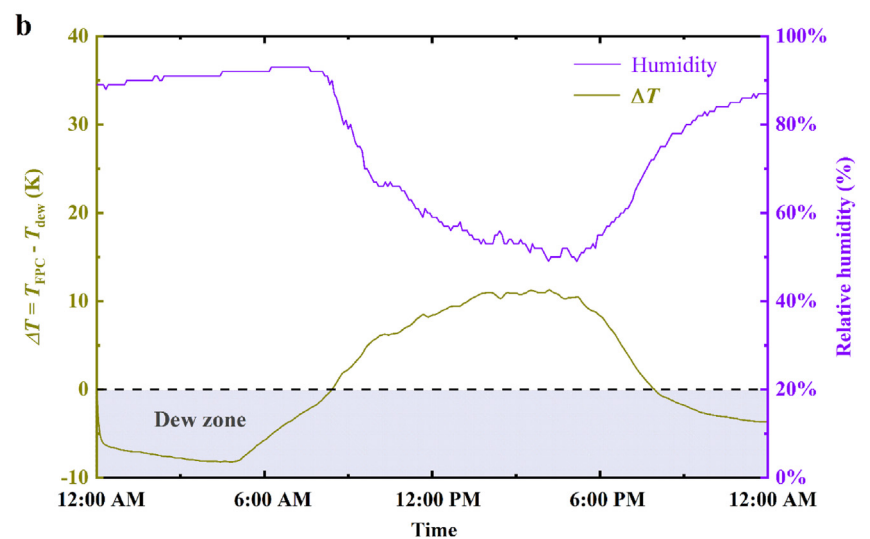


Fig. 4. (a) Thermal performance of the radiative cooling system (black curve) and radiative cooling power (cyan curve) over a 24-h cycle with ambient temperature variation (blue curve). (b) Theoretical dew harvesting potential.

$$Q_{\rm amb}(T_{\rm amb}) = A \int_{0}^{\infty} d\lambda I_{\rm BB}(T_{\rm amb}, \lambda) \varepsilon(\lambda, \theta, \varphi, T_{\rm FPC}) \varepsilon(\lambda, \theta, \varphi)$$
 (4)

where, $\varepsilon(\lambda,\theta,\varphi)$ represents the absorptivity of the atmosphere. Furthermore, $Q_{\text{sum}}(T_{\text{FPC}})$ corresponds to the solar irradiation absorbed by the FPC, as described by:

$$Q_{\text{sun }}(T_{\text{FPC}}) = A \cos \theta_{\text{sun}} \int_{0}^{\infty} d\lambda I_{\text{AM1.5}}(\lambda) \varepsilon(\lambda, \theta_{\text{sun}}, T_{\text{FPC}})$$
 (5)

Here, $I_{\rm AM1.5}(\lambda)$ is the spectral irradiance intensity of solar irradiation at AM 1.5 and $\theta_{\rm sun}$ denotes the direction of the incoming sunlight [37]. The temperature-dependent emissivity of FPC is given as $\varepsilon(\lambda, \theta_{\rm sun}, T_{\rm FPC})$. The time-dependent temperature of the FPC can be obtained by solving the differential equations:

$$C_{\text{FPC}} \frac{dT}{dt} = Q_{\text{total}}(T_{\text{FPC}}, T_{\text{amb}}) \tag{6}$$

where C_{FPC} is the heat capacitance of the FPC. Based on the energy balance equation, the radiative cooling performance of FPC (F1:P1)

is evaluated by calculating the FPC's temperature in response to recorded 24-h outdoor weather data. In this calculation, we use the ambient temperature [40] and solar illumination data [41] on July 20, 2018 in Stanford, California. Fig. 4a shows the temperature change and net radiative cooling power of the FPC as shown in Fig. 2b over a 24-h period. The temperature drop ΔT at sunrise, noon, and sunset remains over 4 K, which promises sufficient radiative cooling effects. The maximum temperature difference is up to 8.4 K, while the net radiative cooling power reaches its maximum of 90 W/m² around 2:15 p.m.

When the passive radiative cooling performance brings the FPC below the dew point temperature of air, water will condense on its surface. To quantify the radiative cooling for dew harvesting under direct sun exposure, we compute the time period for dew harvesting (i.e., $T_{\rm FPC} \leq T_{\rm dew}$) into the day shown in Fig. 4b. Our result shows that our FPC is theoretically able to harvest dew from 12:00 a.m. to 9:00 a.m. and 8:00 p.m. to 12:00 a.m., which indirectly causes the FPC to remain humid during the majority of the passive radiative cooling process due to the hydrophilicity of cellulose fibers in the FPC. To simulate more realistic working conditions, we spray water evenly on the FPC sample using a spray bottle. Here, we create moist states for four FPC samples by spraying different

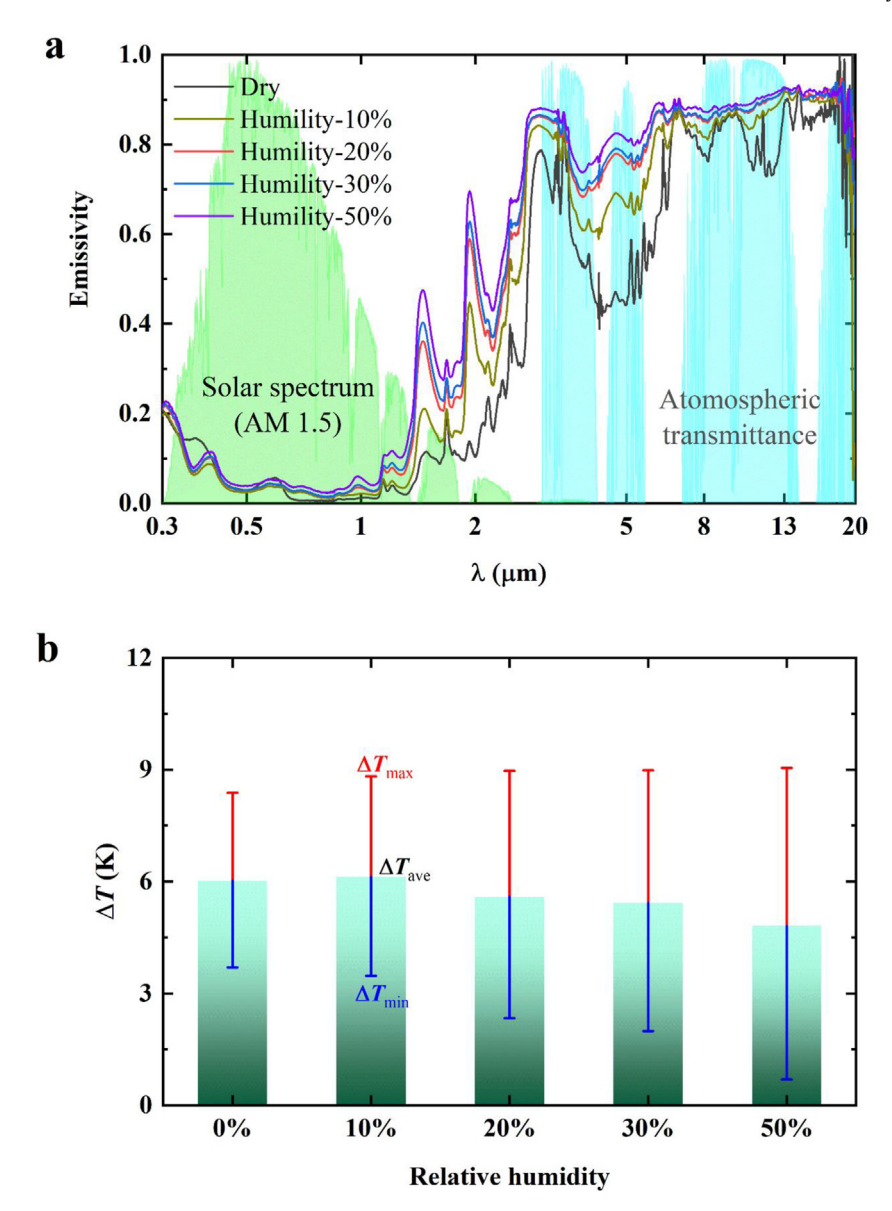


Fig. 5. (a) the comparison of hemispherical spectral emissivities and (b) the calculated temperature difference ($\Delta T = T_{amb} - T_{FPC}$) of 2-mm-thick dry and four humid FPC (F1:P1) samples, respectively.

qualities of DI water, then define the humidity of the FPC sample by the mass ratio of DI water and the FPC sample. One dry FPC sample is also used as a reference. Fig. 5a shows the comparison between the spectral emissivities of the dry and humid FPC samples, respectively. It can be clearly seen that the dew in the PFC greatly increases the mid-IR emissivity but barely affects the solar reflectance, leading to enhanced passive radiative cooling. Based on the above theoretical calculations, the cooling performance of FPC (F1:P1) with various humidities is evaluated, where the humidity is controlled by the amount of water sprayed. The results are shown in Fig. 5b. For a near-ideal situation (completely dry PFC), even with a non-radiative heat transfer coefficient of 8 $\mathrm{Wm}^{-2}\mathrm{K}^{-1}$, a maximum temperature reduction of 8.4 K can be achieved by our FPC under direct sunlight due to the combined high solar reflectivity and strong mid-IR emissivity. Furthermore, the increase in theoretical temperature difference can be enhanced to 9.0 K under direct sunlight with our cooler, which has over 20% humidity due to the emissive contributions of surface water. When the humidity of FPC further increases up to 50%, although the humid FPC can increase its radiative cooling power based on the enhancement of infrared

thermal emissivity within the atmospheric transparent window (8 $\sim 13~\mu m)$, the increased thermal absorptivity in the wavalength range (1 $\sim 2.5~\mu m$) will result in greater temperature difference fluctuations, as shown in Fig. 5b. Besides, we test the anti-fouling property of the FPC in a simulated environment, as seen in Fig. S4. The dry garden soil is employed to attempt to contaminate the FPC. The FPC cannot be dyed by the soil on its surface and is easily blown away without any pollution because of its excellent anti-fouling ability arising from PS foam particles. The weathering durability of the FPCs is also demonstrated by two-month outdoor exposure (including some dust and PM2.5 particles after long-term use), with a little change observed in the spectral solar reflectance and mid-infrared thermal emittance during the atmospheric transparent window (Figs. S5 and S6).

4. Conclusions

In summary, we have demonstrated a facile, low-cost, ecofriendly, and efficient passive radiative cooling material by employing commercially available polystyrene foams and printer papers. Because the fibrous and porous structures have feature sizes comparable to the solar wavelength range, the FPC efficiently scatters solar irradiance. Combining the ultrahigh 96% solar reflectance and 80% emittance of FPC in the infrared wavelength range, we theoretically demonstrate that our proposed FPC can achieve continuous daytime radiative cooling with an average temperature drop of 6 °C under direct sunlight. Even in high humidity, the FPC maintains consistent and effective radiative cooling. This eco-friendly FPC structure advances the application of passive radiative cooling, especially in underdeveloped hot and humid regions. Compared with emerging radiative cooling materials and traditional cooling techniques, our proposed FPC can not only realize efficient passive radiative cooling but also enrich the value of recycled PS foam and decrease environmental pollution.

Credit author statement

Yang Liu: Conceptualization, Data analysis, Writing — original draft, Experimentation design. Xiaojie Liu: Conceptualization, Data analysis. Fangqi Chen: Sample preparation, Experimental measurement. Yanpei Tian: Experimentation design, Data analysis. Andrew Caratenuto: Sample preparation, Experimental measurement. Ying Mu: Experimental measurement. Shuang Cui: Data analysis, Review & editing. Marilyn L. Minus: Data analysis, Review & editing. Yi Zheng: Supervision, Resources, Writing — review & editing.

Declaration of competing interest

The authors declare that they have no known competing financial interests or personal relationships that could have appeared to influence the work reported in this paper.

Data availability

Data will be made available on request.

Acknowledgments

This work was supported in part by the National Science Foundation under Grant No. CBET-1941743 and PHY-1748958.

Appendix A. Supplementary data

Supplementary data to this article can be found online at https://doi.org/10.1016/j.mtsust.2023.100448.

References

- [1] Annual Energy Outlook, 2022. https://www.eia.gov/outlooks/aeo/pdf/ AEO2022_Narrative.pdf.
- [2] P.W. Bridgman, The nature of thermodynamics, in: The Nature of Thermodynamics, Harvard University Press, 2013.
- [3] J.-l. Kou, Z. Jurado, Z. Chen, S. Fan, A.J. Minnich, Daytime radiative cooling using near-black infrared emitters, ACS Photonics 4 (2017) 626–630.
- [4] T. Li, Y. Zhai, S. He, W. Gan, Z. Wei, M. Heidarinejad, D. Dalgo, R. Mi, X. Zhao, J. Song, A radiative cooling structural material, Science 364 (2019) 760–763.
- [5] B. Zhao, M. Hu, X. Ao, N. Chen, G. Pei, Radiative cooling: a review of fundamentals, materials, applications, and prospects, Appl. Energy 236 (2019) 489–513
- [6] J.P. Bijarniya, J. Sarkar, P. Maiti, Review on passive daytime radiative cooling: fundamentals, recent researches, challenges and opportunities, Renew.Sust. Energ. Rev. 133 (2020) 110263.
- [7] X. Yu, J. Chan, C. Chen, Review of radiative cooling materials: performance evaluation and design approaches, Nano Energy 88 (2021) 106259.
- [8] A.P. Raman, M.A. Anoma, L. Zhu, E. Rephaeli, S. Fan, Passive radiative cooling below ambient air temperature under direct sunlight, Nature 515 (2014) 540–544.

- [9] D. Chae, M. Kim, P.-H. Jung, S. Son, J. Seo, Y. Liu, B.J. Lee, H. Lee, Spectrally selective inorganic-based multilayer emitter for daytime radiative cooling, ACS Appl. Mater. Interfaces 12 (2020) 8073–8081.
- [10] Z. Xia, Z. Fang, Z. Zhang, K. Shi, Z. Meng, Easy way to achieve self-adaptive cooling of passive radiative materials, ACS Appl. Mater. Interfaces 12 (2020) 27241–27248.
- [11] N.N. Shi, C.-C. Tsai, F. Camino, G.D. Bernard, N. Yu, R. Wehner, Keeping cool: enhanced optical reflection and radiative heat dissipation in Saharan silver ants. Science 349 (2015) 298–301.
- [12] C. Zou, G. Ren, M.M. Hossain, S. Nirantar, W. Withayachumnankul, T. Ahmed, M. Bhaskaran, S. Sriram, M. Gu, C. Fumeaux, Metal-Loaded dielectric resonator metasurfaces for radiative cooling, Adv. Opt. Mater. 5 (2017) 1700460.
- [13] Y. Tian, X. Liu, Z. Wang, J. Li, Y. Mu, S. Zhou, F. Chen, M.L. Minus, G. Xiao, Y. Zheng, Subambient daytime cooling enabled by hierarchically architected all-inorganic metapaper with enhanced thermal dissipation, Nano Energy 96 (2022) 107085.
- [14] W. Wu, S. Lin, M. Wei, J. Huang, H. Xu, Y. Lu, W. Song, Flexible passive radiative cooling inspired by Saharan silver ants, Sol. Energy Mater. Sol. Cell. 210 (2020) 110512.
- [15] P. Yao, Z. Chen, T. Liu, X. Liao, Z. Yang, J. Li, Y. Jiang, N. Xu, W. Li, B. Zhu, Spider-silk-Inspired nanocomposite polymers for durable daytime radiative cooling, Adv. Mater. (2022) 2208236.
- [16] Y. Zhai, Y. Ma, S.N. David, D. Zhao, R. Lou, G. Tan, R. Yang, X. Yin, Scalable-manufactured randomized glass-polymer hybrid metamaterial for daytime radiative cooling, Science 355 (2017) 1062–1066.
- [17] J. Mandal, Y. Yang, N. Yu, A.P. Raman, Paints as a scalable and effective radiative cooling technology for buildings, Joule 4 (2020) 1350–1356.
- [18] X. Li, J. Peoples, Z. Huang, Z. Zhao, J. Qiu, X. Ruan, Full daytime sub-ambient radiative cooling in commercial-like paints with high figure of merit, Cell Reports Physical Science 1 (2020) 100221.
- [19] X. Li, J. Peoples, P. Yao, X. Ruan, Ultrawhite BaSO4 paints and films for remarkable daytime subambient radiative cooling, ACS Appl. Mater. Interfaces 13 (2021) 21733–21739.
- [20] X. Wang, X. Liu, Z. Li, H. Zhang, Z. Yang, H. Zhou, T. Fan, Scalable flexible hybrid membranes with photonic structures for daytime radiative cooling, Adv. Funct. Mater. 30 (2020) 1907562.
- [21] Y. Tian, H. Shao, X. Liu, F. Chen, Y. Li, C. Tang, Y. Zheng, Superhydrophobic and recyclable cellulose-fiber-based composites for high-efficiency passive radiative cooling, ACS Appl. Mater. Interfaces 13 (2021) 22521–22530.
- [22] R. Zhu, D. Hu, Z. Chen, X. Xu, Y. Zou, L. Wang, Y. Gu, Plasmon-enhanced infrared emission approaching the theoretical limit of radiative cooling ability, Nano Lett. 20 (2020) 6974–6980.
- [23] J. Mandal, Y. Fu, A.C. Overvig, M. Jia, K. Sun, N.N. Shi, H. Zhou, X. Xiao, N. Yu, Y. Yang, Hierarchically porous polymer coatings for highly efficient passive daytime radiative cooling, Science 362 (2018) 315–319.
- [24] H. Zhao, Q. Sun, J. Zhou, X. Deng, J. Cui, Switchable cavitation in silicone coatings for energy-saving cooling and heating, Adv. Mater. 32 (2020) 2000870.
- [25] D. Li, X. Liu, W. Li, Z. Lin, B. Zhu, Z. Li, J. Li, B. Li, S. Fan, J. Xie, Scalable and hierarchically designed polymer film as a selective thermal emitter for high-performance all-day radiative cooling, Nat. Nanotechnol. 16 (2021) 153–158.
- [26] L. Zhou, J. Zhao, H. Huang, F. Nan, G. Zhou, Q. Ou, Flexible polymer photonic films with embedded microvoids for high-performance passive daytime radiative cooling, ACS Photonics 8 (2021) 3301–3307.
- [27] T. Wang, Y. Wu, L. Shi, X. Hu, M. Chen, L. Wu, A structural polymer for highly efficient all-day passive radiative cooling, Nat. Commun. 12 (2021) 365.
- [28] J. Li, Y. Liang, W. Li, N. Xu, B. Zhu, Z. Wu, X. Wang, S. Fan, M. Wang, J. Zhu, Protecting ice from melting under sunlight via radiative cooling, Sci. Adv. 8 (2022) eabi9756.
- [29] Z.O. Schyns, M.P. Shaver, Mechanical recycling of packaging plastics: a review, Macromol. Rapid Commun. 42 (2021) 2000415.
- [30] J. Di, B.K. Reck, A. Miatto, T.E. Graedel, United States plastics: large flows, short lifetimes, and negligible recycling, Resour. Conserv. Recycl. 167 (2021) 105440.
- [31] S. Thakur, A. Verma, B. Sharma, J. Chaudhary, S. Tamulevicius, V.K. Thakur, Recent developments in recycling of polystyrene based plastics, Curr. Opin. Green Sustain. Chem. 13 (2018) 32–38.
- [32] L.D. Ellis, N.A. Rorrer, K.P. Sullivan, M. Otto, J.E. McGeehan, Y. Román-Leshkov, N. Wierckx, G.T. Beckham, Chemical and biological catalysis for plastics recycling and upcycling, Nat. Catal. 4 (2021) 539-556.
- [33] J.C. Worch, A.P. Dove, 100th Anniversary of macromolecular science view-point: toward catalytic chemical recycling of waste (and future) plastics, ACS Macro Lett. 9 (2020) 1494–1506.
- [34] G. Faraca, T. Astrup, Plastic waste from recycling centres: characterisation and evaluation of plastic recyclability, Waste Manage. (Tucson, Ariz.) 95 (2019) 388–398
- [35] M. Ono, K. Chen, W. Li, S. Fan, Self-adaptive radiative cooling based on phase change materials, Opt Express 26 (2018) A777—A787.
- [36] P. Yang, C. Chen, Z.M. Zhang, A dual-layer structure with record-high solar reflectance for daytime radiative cooling, Sol. Energy 169 (2018) 316–324.
- [37] S. Fan, W. Li, Photonics and thermodynamics concepts in radiative cooling, Nat. Photonics (2022) 1–9.

- [38] Y. Tian, L. Qian, X. Liu, A. Ghanekar, G. Xiao, Y. Zheng, Highly effective photon-to-cooling thermal device, Sci. Rep. 9 (2019) 1–11.
 [39] X. Liu, Y. Tian, F. Chen, A. Ghanekar, M. Antezza, Y. Zheng, Continuously variable emission for mechanical deformation induced radiative cooling, Communications Materials 1 (2020) 1–7.
- [40] Weather Underground, https://www.wunderground.com/dashboard/pws/KCASTANF2/graph/2018-07-20/2018-07-20/daily.
 [41] Calculation of Solar Insolation, https://www.pveducation.org/pvcdrom/properties-of-sunlight/calculation-of-solar-insolation.